

Di-photon versus di-hadron correlations in p+A collisions

Alex Kovner¹ and Amir H. Rezaeian^{2,3,a}

¹*Dept. of Physics, University of Connecticut, High, Storrs, CT 06269, USA*

²*Departamento de Física, Universidad Técnica Federico Santa María, Avda. España 1680, Casilla 110-V, Valparaíso, Chile*

³*Centro Científico Tecnológico de Valparaíso (CCTVal), Universidad Técnica Federico Santa María, Casilla 110-V, Valparaíso, Chile*

Abstract. We study the di-photon correlations in quark-nucleus and proton-nucleus collisions at RHIC and the LHC. We show that the single fragmentation di-photon produces the away side correlations peak, and the double fragmentation component of prompt di-photon is responsible for the near-side peak, and the long-range in rapidity near-side azimuthal collimation, the so-called "ridge" structure. We show that while di-photon ridge exists at the LHC in quark-nucleus collisions, the effect disappears in proton-nucleus collisions at the LHC. We show that the di-photon correlation measurements in p+A collisions can help to discriminate among models and understand the true origin of the observed di-hadron ridge in p+A collisions.

1 Introduction

It is believed that prompt photons, do not participate in the final-state interactions and can be considered as a golden channel to probe intrinsic correlations of partons in the hadronic and nuclear wavefunctions. Moreover, in contrast to gluons (and hadrons) production, prompt photons do not scatter on the target gluon field, but rather decohere from the projectile wavefunction due to scattering of the quarks, see Fig. 1. In this sense, the underlying mechanism of di-photon and di-hadron productions are quite different and di-photon can provide vital information to address whether it is the initial or final state effects that play dominant role in formation of the ridge collimation in p+p(A) collisions.

The observation of the so-called ridge phenomenon, namely the long-range in rapidity near-side ($\Delta\phi \approx 0$) di-hadron correlations in high-multiplicity events selection in both proton-proton (p+p) and proton (duetron)+nucleus collisions at the LHC and RHIC [1], triggered an on-going hot debate about the underlying dynamics of high-multiplicity events. It is an open question whether the ridge phenomenon in p+p(A) collisions mainly come from initial-state Color-Glass-Condensate (CGC) [2–6] or final-state hydrodynamic [7] approaches. Another interesting question is that if the ridge is a universal phenomenon, for all different two-particle productions such as two photons production in p+p(A) collisions.

^ae-mail: Amir.Rezaeian@usm.cl

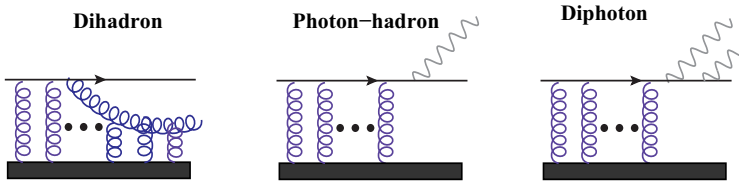


Figure 1. Typical CGC diagrams contributing to the inclusive gluon-quark (left), photon-quark (center) and prompt di-photon-quark (right) production at leading-order in proton-nucleus collisions.

2 Main formulation: the factorization

The inclusive prompt di-photon production $h + A \rightarrow \gamma_1 + \gamma_2 + X$ in high-energy dilute-dense scatterings was recently calculated in the CGC approach [8, 9] where in the leading order approximation, at forward rapidity, a valence quark of the projectile hadron emits two photons with momenta k_1 and k_2 via Bremsstrahlung and the produced di-photon+jet is then put on shell by interacting coherently over the whole longitudinal extent of the target, see Fig. 1. The inclusive di-photon differential cross-section at leading-log approximation can be written in the following factorization form [8, 9],

$$\frac{d\sigma^{pA \rightarrow \gamma(k_1)\gamma(k_2)X}}{d^2\mathbf{k}_1 d^2\mathbf{k}_2 d\eta_1 d\eta_2} = \alpha_{em}^2 \int_{x_q^{min}}^1 dx_q f(x_q, \mu_T^2) \int d^2\mathbf{l}_T \mathcal{H}(\mathbf{k}_{1T}, \mathbf{k}_{2T}, \mathbf{l}_T, \zeta_1, \zeta_2) N_F(l_T, x_g), \quad (1)$$

where the function $N_F(l_T, x_g)$ is the correlator of two light-like fundamental Wilson lines in the background of the color fields of the target, and it encodes the small- x dynamics of the target. The dipole amplitude $N_F(l_T, x_g)$ depends on the total transfer transverse momentum to target l_T and the fraction of light-cone momentum of target taken away by the exchange gluons x_g . At large N_c the dipole amplitude is obtained via the Balitsky-Kovchegov evolution equation [10]. The matrix function \mathcal{H} depends on the transverse momenta of produced photons \mathbf{k}_{1T} , \mathbf{k}_{2T} and the light-cone fractions of momentum of projectile taken away by two photons ζ_1, ζ_2 . The matrix functional \mathcal{H} is fairly lengthy and can be found in Ref. [9]. In Eq. (1), $f_q(x_q, \mu_T^2)$ denotes the parton distributions function (PDF) in the projectile hadron which depends on factorization scale μ and the parameter x_q defined as the ratio of the incoming quark to the projectile nucleon energy. The summation over quark and anti-quark flavor is implicit in Eq. (1). The matrix functional \mathcal{H} includes the single and double fragmentation photon contributions, corresponding to the kinematics where only one emitted photon or both emitted photons are almost collinear with the outgoing quark. Note that both single and double fragmentation di-photon contributions, as well direct di-photon part are sensitive to the saturation dynamics via a convolution with the dipole amplitude $N_F(l_T, x_g)$, see Eq. (1). The lower limit of integral x_q^{min} in the factorization Eq. (1) and light-cone variables x_g, ζ_1, ζ_2 are obtained via the energy-momentum conservation relations [8, 9].

The azimuthal correlation of the produced di-photon is defined via

$$C_2(\Delta\phi, k_{1T}, k_{2T}, \eta_1, \eta_2) = \frac{d\sigma^{pA \rightarrow \gamma(k_1)\gamma(k_2)X}}{d^2\mathbf{k}_{1T} d\eta_{\gamma_1} d^2\mathbf{k}_{2T} d\eta_{\gamma_2}} [\Delta\phi] / \int_0^{2\pi} d\Delta\phi \frac{d\sigma^{pA \rightarrow \gamma(k_1)\gamma(k_2)X}}{d^2\mathbf{k}_{1T} d\eta_{\gamma_1} d^2\mathbf{k}_{2T} d\eta_{\gamma_2}} - C_{ZYAM}, \quad (2)$$

where $\Delta\phi$ denotes the azimuthal angle between the two produced photons in the plane transverse to the collision axis.

In our hybrid approach for di-photon production [8, 9], the projectile proton is assumed to be in dilute regime (as one may expect to be so at forward rapidities) and is consequently treated in standard

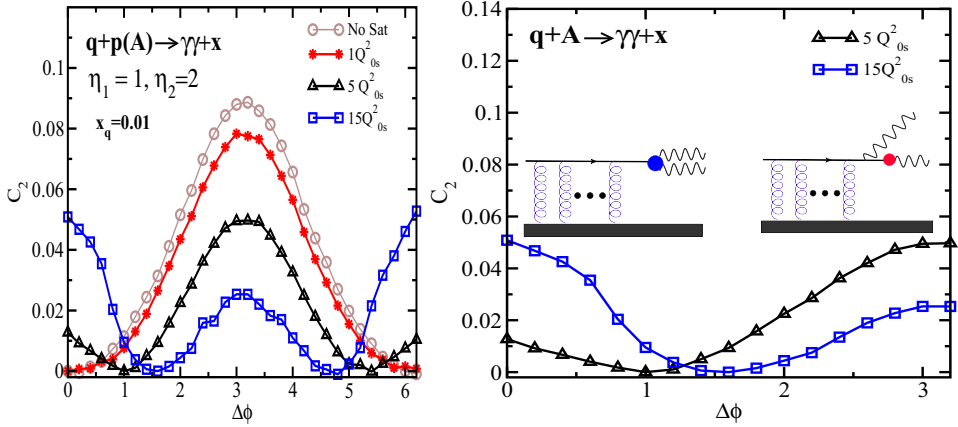


Figure 2. Prompt di-photon correlations C_2 as a function of angle between two photons $\Delta\phi$ in q+Pb collisions at the LHC ($\sqrt{s} = 5.02$ TeV) with $\eta_1 = 1, \eta_2 = 2$ and $x_q = 0.01$ at different initial saturation scales (corresponding to different centralities). A schematic contribution of different typical CGC diagrams to the double inclusive prompt photon production at different angle is also shown. The plots are taken from [9].

parton model approach, while the target is treated as a CGC object at forward rapidities. Therefore, we have here only one saturation scale. This is one of main differences between our approach and the approach of Ref. [5] where the existence of two saturation scales in the problem (for the projectile proton and the target) in p+Pb collisions at forward rapidities, is essential in order to find a good fit to the di-hadron ridge data.

3 Results and Conclusion

In Fig. 2, we show the initial saturation scale dependence of C_2 at a fixed $x_q = 0.01$ in q+p(A) collisions at 5.02 TeV with rapidities of the produced photon $\eta_1 = 1$ and $\eta_2 = 2$. The effect of size and density of the target is simulated by taking different initial saturation scale for the running-coupling BK (rcBK) evolution equation. Namely we use the different solutions of the rcBK evolution equation with different initial saturation scales for the target $Q_{0s,A}^2 = NQ_{0s}^2$ and $N = 1, 5, 15$. We recall that an initial saturation scale Q_{0s} describes a proton target in minimum-bias electron-proton or proton-proton collisions [12], while an initial saturation scale of about $5 \div 7Q_{0s}$ describes a heavy nuclear target in minimum-bias proton-nucleus collisions [11]. We also compare with the non-saturation model (labeled by "No Sat" in the plot). It is seen that increasing the saturation scale in the system increases the near-side correlations leading to near-side collimation, while it decreases away-side correlation leading to the away-side decorrelation. Note that if momentum transfer from the target is small enough, the photon collinear to the outgoing quark, and the photon emerging from the initial photon-quark state have opposite transverse momenta, leading to back-to-back correlation at $\Delta\phi = \pi$ due to the single fragmentation di-photon contribution. Now increasing the exchanges to the target by increasing the saturation scale, unbalances the back-to-back correlations. The double fragmentation and direct di-photon contributions on the other hand, are restricted to kinematics where the transverse momentum of the outgoing quark jet is relatively large. By increasing the saturation scale, the main

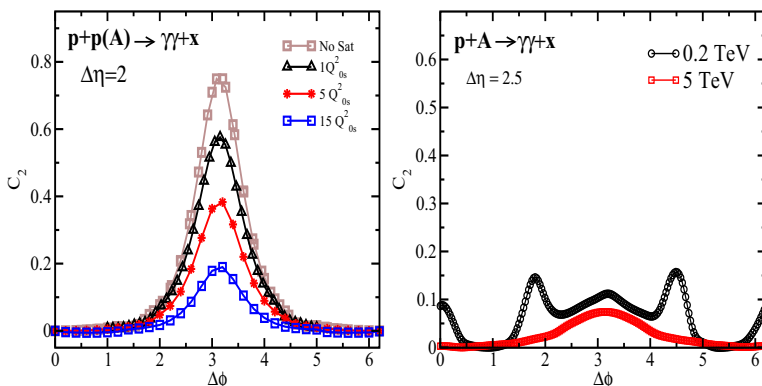


Figure 3. Left: The initial-saturation-scale dependence of prompt di-photon correlations C_2 in p+p(A) collisions at the LHC 5.02 TeV. Right: Comparison of C_2 at RHIC and the LHC for fixed transverse momenta of di-photon at $k_{1T} = k_{2T} = 1$ GeV with $\eta_1 = 1$ and $\eta_2 = 3.5$ in minimum-bias p+A collisions. The plots are taken from [9].

contributions of integrand is shifted to higher transverse momentum, leading to the enhancement of double-fragmentation contributions at the near-side $\Delta\phi = 0$.

In order to compute the correlations in proton-nucleus collisions, we should convolute the partonic cross-section with the PDFs of quarks and anti-quarks, and perform the integral over x_q , see Eq. (1). Note that the near-side and away-side correlations are enhanced by decreasing x_q light-cone variable. For a large x_q , all correlations both at near-side and away-side disappear, albeit this effect is more pronounced for the near-side correlations [9]. Therefore, a priori, it is not obvious how the integration over x_q will affect the di-photon correlations in p+A collisions. In Fig. 3, we show the initial-saturation-scale dependence of prompt di-photon correlations defined via C_2 in p+p(A) collisions at 5.02 TeV and $\eta_1 = 1$, $\eta_2 = 3$ with fixed transverse momenta of photons $k_{1T} = k_{2T} = 2$ GeV. It is seen at the LHC energy 5.02 TeV while the away-side correlation decreases by increasing the saturation scale, the near-side correlations defined via Eq. (2) almost disappears at all different centralities (corresponding to different saturation scales). In Fig. 3, we also compare the correlation C_2 at RHIC and the LHC at fixed transverse momenta of di-photon $k_{1T} = k_{2T} = 1$ GeV with rapidities $\eta_1 = 1$ and $\eta_2 = 3.5$ in minimum-bias proton-nucleus collisions. It is interesting that at RHIC in stark contrast to the LHC, a ridge-like structure appears at low transverse momentum of the produced photons $0.2 < k_T[\text{GeV}] < 3$. The near-side collimation at RHIC survives up to rapidity interval $\Delta\eta \approx 3$. It is also seen in Fig. 3 that the prompt di-photon correlations at forward rapidities in the away side region exhibit single or double peak structure depending on the kinematics. The double-peak structure is universal feature of Electromagnetic probes [9] and similar effect was also reported for photon-hadron [13] and dilepton-hadron [14] correlations in high-energy p+Pb collisions. This feature more clearly shows up at RHIC energy [9, 13, 14].

To conclude: we showed that in high-energy collisions, prompt di-photon production exhibits long-range correlations in quark-nucleus collisions at RHIC and the LHC albeit the physics of these correlations is significantly different than that of di-hadron correlations discussed previously [2–6] in the CGC framework. In particular, the correlations decrease for moderate rapidity separation between the two photons about $\Delta\eta \approx 1 \div 3$. We found that di-photon correlations defined via Eq. (2) exhibits ridge-like structure at low transverse momenta in p+A collisions at RHIC while this effect disappears in p+A collisions at the LHC 5.02 TeV. We showed that away-side di-photon de-correlations

by increasing the saturation scale is somehow similar to the di-hadron de-correlations observed at the RHIC [15], see also Ref. [16]. However, di-photon correlations can exhibit double-peak structure at away-side which is a unique feature of Electromagnetic probes [9, 13, 14].

Acknowledgements The work of A.H.R. is supported in part by Fondecyt grant 1150135.

References

- [1] V. Khachatryan *et al.* (CMS Collaboration), JHEP **09**, 091 (2010); S. Chatrchyan *et al.* (CMS Collaboration), Phys. Lett. **B718**, 795 (2013); B. Abelev *et al.* (ALICE Collaboration), Phys. Lett. **B719**, 29 (2013); G. Aad *et al.* (ATLAS Collaboration), Phys. Rev. Lett. **110**, 182302 (2013); B. B. Abelev *et al.* (ALICE Collaboration), Phys. Lett. **B726**, 164 (2013); A. Adare *et al.* (PHENIX Collaboration), Phys. Rev. Lett. **111**, 212301 (2013), 1303.1794; L. Adamczyk *et al.* (STAR Collaboration) (2014), accepted by Phys. Lett.B, 1412.8437; 1502.07652.
- [2] A. Dumitru, K. Dusling, F. Gelis, J. Jalilian-Marian, T. Lappi and Venugopalan, Phys. Lett. **B697**, 21 (2011).
- [3] A. Kovner and M. Lublinsky, Phys. Rev. **D83**, 034017 (2011).
- [4] E. Levin and A. H. Rezaeian, Phys. Rev. **D84**, 034031 (2011).
- [5] K. Dusling and R. Venugopalan, Phys. Rev. **D87**, 094034 (2013); **D87**, 054014 (2013).
- [6] A. Kovner and M. Lublinsky, Int. J. Mod. Phys. **E22**, 1330001 (2013) and references therein.
- [7] P. Bozek, Eur. Phys. J. **C71**, 1530 (2011); Phys. Rev. **C88**, 014903 (2013); P. Bozek and W. Broniowski, Phys. Lett. **B718**, 1557 (2013); P. Bozek, W. Broniowski and G. Torrieri, Phys. Rev. Lett. **111**, 172303 (2013).
- [8] A. Kovner and A. H. Rezaeian, Phys. Rev. **D90**, 014031 (2014).
- [9] A. Kovner and A. H. Rezaeian, Phys. Rev. **D92**, 074045 (2015), arXiv:1508.02412.
- [10] I. Balitsky, Nucl. Phys. **B463**, 99 (1996); Y. V. Kovchegov, Phys. Rev. **D60**, 034008 (1999); Phys. Rev. **D61**, 074018 (2000).
- [11] A. H. Rezaeian, Phys. Lett. **B718**, 1058 (2013); J. Jalilian-Marian and A. H. Rezaeian, Phys. Rev. **D85**, 014017 (2012); E. Levin and A. H. Rezaeian, Phys. Rev. **D82**, 014022 (2010); Phys. Rev. **D82**, 054003 (2010); Phys. Rev. **D83**, 114001 (2011); A. H. Rezaeian, Phys. Rev. **D85**, 014028 (2012); A. H. Rezaeian, M. Siddikov, M. Van de Klundert and R. Venugopalan, Phys. Rev. **D87**, 034002 (2013); A. H. Rezaeian and I. Schmidt, Phys. Rev. **D88**, 074016 (2013); N. Armesto and A. H. Rezaeian, Phys. Rev. **D90**, 054003 (2014); A. H. Rezaeian, Phys. Lett. **B727**, 218 (2013).
- [12] J. L. Albacete, N. Armesto, J. G. Milhano, P. Quiroga Arias and C. A. Salgado, Eur. Phys. J. **C71**, 1705 (2011).
- [13] A. H. Rezaeian, Phys. Rev. **D86**, 094016 (2012); J. Jalilian-Marian and A. H. Rezaeian, Phys. Rev. **D86**, 034016 (2012).
- [14] A. Stasto, B-W. Xiao and D. Zaslavsky, Phys. Rev. **D86**, 014009 (2012).
- [15] A. Adare *et al.* [PHENIX Collaboration], Phys. Rev. Lett. **107**, 172301 (2011); E. Braidot, for the STAR Collaboration, Nucl. Phys. **A854**, 168 (2011); E. Braidot, Ph.D. thesis, arXiv:1102.0931.
- [16] J. L. Albacete and C. Marquet, Phys. Rev. Lett. **105**, 162301 (2010).